Dynamic computations of nonlinear beams in contact with rough surfaces

Denis Duhamel, Trong Dai Vu, Zouhir Abbadi, Hai-Ping Yin, Arnaud Gaudin

Dynamic computations of nonlinear beams in contact with rough surfaces

Denis Duhamel[a,*], Trong Dai Vu[a,b], Zouhir Abbadi[b], Hai-Ping Yin[a], Arnaud Gaudin[b]

[a] *Université Paris-Est, Laboratoire Navier, ENPC/IFSTTAR/CNRS, 6 et 8 Avenue Blaise Pascal, Cité Descartes, Champs sur Marne, 77455 Marne la Vallée, cedex 2, France*
[b] *PSA Peugeot Citroën, Automotive Research and Advanced Engineering Division, Centre Technique de Vélizy A, Route de Gisy - cc vv1415, 78943 Vélizy-Villacoublay, France*

Abstract

We present computations of a two-dimensional nonlinear ring in contact with a rough surface for the analysis of tire dynamic behaviour at low frequencies in both non-rolling and rolling conditions. For the ring, the assumptions of a Timoshenko beam and finite displacements are considered to build the model. The analytical formulation is established successfully in linear/nonlinear static and dynamic states in non-rolling and rolling conditions using an Arbitrary Lagrangian Eulerian approach. Then, the contact with a real road is introduced. In particular, the calculation of the contact is divided into a non-linear stationary analysis followed by a linear dynamic calculation. The validation of this model is successfully done by comparisons with test results like rolling on simple shapes or with Abaqus computations.

Keywords: tire; vibration; non linear; beam; noise; contact; rough surface

1. Introduction

The interior noise of vehicles has an important source coming from tires in the low frequency range, typically up to 400Hz. For these frequencies the rolling noise is mainly due to tire vibrations. These vibrations are themselves created by the unsteady contact between road asperities and the tire tread pattern. For predicting this noise generation a tire model is necessary. In the past, various tire models have been developed focusing on different aspects of the problem.

A first class of models is the two and three-dimensional circular ring models. For instance Böhm [1], Heckl [2] and Kropp [3] have modelled the tread as a circular Euler-Bernoulli beam. Sidewalls are represented by radial and tangential springs. This model takes into account the effect of the internal pressure and is linear. These circular ring models are very useful for analysing the radial vibrations of tires for low frequencies. Several authors added the effect of rotation, see for instance Meftah [4], Périsse [5] and Campanac [6, 7]. In addition, Huang [8] has analysed the rotating ring model under a suspension system. So, two-dimensional circular ring models allow the modelling of the dynamic behaviour of tires for low frequencies [0-400Hz] and analytical transfer functions can be obtained to deal with contact problems. All these models are linear and do not allow to consider, for instance, the influence of the vehicle load or nonlinear material behaviours on tire vibrations. For higher frequencies, plates models were developed by [9–12]. Regarding three-dimensional numerical models, Fadavi [13] and Brinkmeier [14] used Abaqus to model a tire. Another possibility is to use waveguides as in Waki [15] or Duhamel [16, 17].

*Corresponding author. Tel.: +33 1 64 15 37 28 ; fax: +33 1 64 15 37 41.
E-mail address: denis.duhamel@enpc.fr

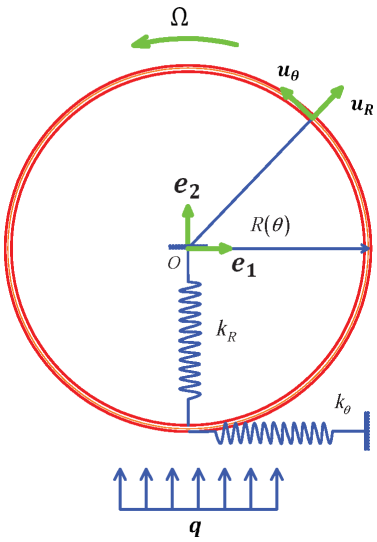

Figure 1: Description of the circular ring model

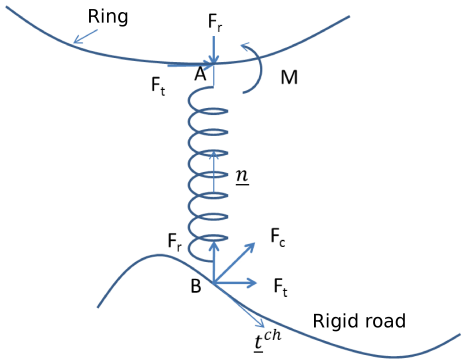

Figure 2: Contact forces

Often, authors have neglected the quasi-static deformation of tires and confused the stationary configuration with the configuration of reference. Under the load of the vehicle and the effect of the air pressure, tires undergo nonlinear deformations. It is thus necessary to distinguish the non-deformed and deformed configurations. This configuration is not known and is obtained by solving the equilibrium equations in stationary regime. This point was for instance developed by [18–20] which used a FEM model for computing the response of tires including the quasi-static deformation and gyroscopic effects. However, these FEM models leads to heavy computations.

This paper aims at developing a nonlinear circular ring model with a good representation of shear deformations to get a mostly analytical model able to estimate the influence of non linearities and to use it for solving contact problems with a rough surface. The structure of the paper is the following. In section two a Timoshenko beam model including shear and rotating effects with large deformations is considered. In section three the contact model is developed. Finally, in section four, examples and validations are given before a conclusion.

2. Beam in finite transformation

The description of the circular ring model representing a tire is illustrated in figure (1). The tread is described as a circular beam. The sides are modelled using radial and tangential springs with respective stiffness k_R, k_θ. The pressure is modelled as a uniform load on the ring. The circular ring has a radius R, a straight section A and a thickness e. The beam is assumed very thin with $\frac{e}{R} \ll 1$.

Each material point in the rotating configuration is defined by two variables (z, θ) in the polar coordinates defined by $(\boldsymbol{u}_R, \boldsymbol{u}_\theta)$ with z varying in the range $[-\frac{e}{2}; \frac{e}{2}]$ and θ in $[0; 2\pi]$. In the rotating configuration, a material point can be represented in the following way:

$$\boldsymbol{OP} = \boldsymbol{OS} + \boldsymbol{SP} = (R + z)\boldsymbol{u}_R \tag{1}$$

with S is a point on the neutral fibre of the beam. S and P belong to the same section. Four configurations are defined: the reference configuration, the rigid rotating configuration, the stationary configuration (rolling on a flat road) and the final configuration (time dependent vibration of the ring). They are referred in the following with indices 0, r, s and t respectively. By switching to the stationary configuration, a displacement field is applied so that $P \to P'$ and $S \to S'$. Point S moves to point S' by two translations $(u(\theta), w(\theta))$.

Point P turns by an angle α to point P'. So a Timoshenko beam model is used. The displacement vector of a material point is:

$$\boldsymbol{u} = \boldsymbol{OP'} - \boldsymbol{OP} = (u + z(\cos\alpha - 1))\boldsymbol{u}_R + (w + z\sin\alpha)\boldsymbol{u}_\theta \tag{2}$$

and the strain tensor of the transformation is computed by $\boldsymbol{e} = \frac{1}{2}({}^T\boldsymbol{F}.\boldsymbol{F} - \boldsymbol{I})$, whose components are:

$$\begin{aligned} e_{RR} &= 0 \\ e_{R\theta} &= e_{\theta R} = \frac{1}{2R}\left(\zeta^2 - \zeta + 1\right)\left((u' - w)\cos\alpha + (R + u + w')\sin\alpha\right) \\ e_{\theta\theta} &= \frac{1 - 2\zeta + 3\zeta^2}{2R^2}\Big((u' - w)^2 + (R + u + w')^2 + 2R\zeta\left(\alpha' + 1\right)\left((R + u + w')\cos\alpha - (u' - w)\sin\alpha\right)\Big) \\ &\quad + R^2\zeta^2\left(\alpha' + 1\right)^2\Big) - \frac{1}{2} \end{aligned} \tag{3}$$

with $\zeta = z/R$.

Material behaviour of the elastic ring is assumed linear elastic. The stress tensor can be written with the engineering notations as:

$$\begin{pmatrix} S_{\theta\theta} \\ S_{R\theta} \end{pmatrix} = \begin{pmatrix} E & 0 \\ 0 & G \end{pmatrix} \begin{pmatrix} e_{\theta\theta} \\ 2e_{R\theta} \end{pmatrix} \tag{4}$$

with E and G are the Young and shear modulus. Active forces on the cross section are the normal force N, the shear force V and the moment M, which are calculated in the reference configuration $(\boldsymbol{u}_R, \boldsymbol{u}_\theta)$ by $N = \int\limits_A S_{\theta\theta}dA,\ V = \int\limits_A S_{R\theta}dA,\ M = \int\limits_A zS_{\theta\theta}dA$ with A is the cross-section area.

In our case, different forces are applied on the ring and consist of the air pressure, the contact force and the reactions of springs. Air pressure results in a pressure p uniform along the ring. For the nonlinear case, the pressure follows the deformation and is given by $\boldsymbol{p} = -p\boldsymbol{Oz} \wedge \left(\frac{\partial \boldsymbol{OS'}}{R\partial\theta}\right)$. At first, the tire/road contact is simply modelled by a point force in the radial direction $\begin{pmatrix} f_R \\ 0 \end{pmatrix}$. The forces of the springs are given by $\begin{pmatrix} f_R^{spring} = k_R.u \\ f_\theta^{spring} = k_\theta.w \end{pmatrix}$. The components $(f_R^{spring}, f_\theta^{spring})$ are respectively in the direction of $\boldsymbol{u}_R$ and $\boldsymbol{u}_\theta$ in the case of linear deformation and follow the deformation of the neutral axis for the nonlinear case.

The equations of equilibrium are finally given by (see [21] for details):

$$\begin{aligned} &\frac{1}{R}\Big(V_t'\cos\alpha - N_t'\sin\alpha - \alpha_t'\left(V\sin\alpha + N\cos\alpha\right)\Big) + p\frac{u_t + w_t'}{R} + p_t\frac{R + u + w'}{R} - \frac{\alpha_t}{R}\left(V'\sin\alpha + N'\cos\alpha\right) \\ &-\frac{\alpha' + 1}{R}\Big(V_t\sin\alpha + N_t\cos\alpha + \alpha_t\left(V\cos\alpha - N\sin\alpha\right)\Big) + {f_R}^t - k_R u_t - \rho\Omega^2 A\left(u_t'' - 2w_t' - u_t\right) = \rho A\ddot{u}_t + 2\rho\Omega A\left(\dot{u}_t' - \dot{w}_t\right) \\ &\frac{1}{R}\Big(V_t'\sin\alpha + N_t'\cos\alpha + \alpha_t'\left(V\cos\alpha - N\sin\alpha\right)\Big) - p\frac{u_t' - w_t}{R} - p_t\frac{u' - w}{R} + \frac{\alpha_t}{R}\left(V'\cos\alpha - N'\sin\alpha\right) \\ &+\frac{\alpha' + 1}{R}\Big(V_t\cos\alpha - N_t\sin\alpha - \alpha_t\left(N\cos\alpha + V\sin\alpha\right)\Big) - k_\theta w - \rho\Omega^2 A\left(w_t'' + 2u_t' - w_t\right) = \rho A\ddot{w}_t + 2\rho\Omega A\left(\dot{u}_t + \dot{w}_t'\right) \\ &\frac{1}{R}M_t' + \frac{1}{R}\Big(\left(u_t' - w_t\right)\left(V\sin\alpha + N\cos\alpha\right) - \left(u_t + w_t'\right)\left(V\cos\alpha - N\sin\alpha\right)\Big) + \\ &\frac{1}{R}\Big(\left(u' - w\right)\left(V_t\sin\alpha + N_t\cos\alpha\right) - \left(R + u + w'\right)\left(V_t\cos\alpha - N_t\sin\alpha\right)\Big) + \\ &\frac{1}{R}\Big(\alpha_t\left(u' - w\right)\left(V\cos\alpha - N\sin\alpha\right) + \alpha_t\left(R + u + w'\right)\left(V\sin\alpha + N\cos\alpha\right)\Big) - \rho\Omega^2 I\alpha_t'' = \rho I\ddot{\alpha}_t + 2\rho\Omega I\dot{\alpha}_t' \end{aligned} \tag{5}$$

with Ω is the rotation speed, I the inertia of the cross-section and the forces and displacements are decomposed into a stationary part, without index, and a time dependent linear perturbation with indices t. This system can be put under the form:

$$\boldsymbol{M}\,\ddot{\boldsymbol{u}}_t + \boldsymbol{C}\,\dot{\boldsymbol{u}}_t + \boldsymbol{K}\,\boldsymbol{u}_t = \boldsymbol{f}_t \tag{6}$$

with

$$\boldsymbol{K} = \frac{\partial \boldsymbol{g}}{\partial \boldsymbol{u}_s} \tag{7}$$

if the stationary equilibrium equations are written under the form:

$$\boldsymbol{g}(\boldsymbol{u}_s) = \boldsymbol{f}_s \tag{8}$$

with $\boldsymbol{g}$ represents the function of the internal forces in the beam. The mass matrix $\boldsymbol{M}$ and the gyroscopic matrix $\boldsymbol{C}$ are easily constructed by discretizing their respective terms in the dynamic equation (5).

3. Contact with a rough surface

It is assumed that the springs can be lengthened or shortened only in the direction normal to the surface of the ring and that the stiffness of the springs represents that of the rubber pads (see figure 2). If the i^{th} point on the pad is in contact, the spring is compressed by δl_i. The displacement of the i^{th} point on the ring always has the expression $\underline{u}_i = u_{Xi}\underline{e}_X + u_{Zi}\underline{e}_Z$. But we must add the deformation of the pads (of original length l_0):

$$\begin{array}{l} x_{li} = X_i + u_{Xi} + (l_0 - \delta l_i)\,\underline{n}_i.\underline{e}_X \\ z_{li} = Z_i + u_{Zi} + (l_0 - \delta l_i)\,\underline{n}_i.\underline{e}_Z \end{array} \tag{9}$$

The geometrical condition of the contact is given by the following relation:

$$z_{li} = f_{ch}(x_{li}) \tag{10}$$

with the profile of the road described by the function $f_{ch}(x_{li})$. The contact force is decomposed in two directions:

$$\underline{F}_c = F_r\,\underline{n} + F_t\,(\underline{n} \wedge \underline{e}_Y) \tag{11}$$

Where $\underline{n}$ is the unit vector in the direction of the deformed spring and $\underline{e}_Y = \underline{e}_Z \wedge \underline{e}_X$. The frictionless contact hypothesis leads to $\underline{F}_c.\underline{t}^{ch} = 0$ with $\underline{t}^{ch}$ the tangential vector of the road at the point of contact (x_{li}, z_{li}) given by $\underline{t}^{ch} = \underline{e}_X + \frac{df_{ch}}{dx}(x_{li})\underline{e}_Z$

The forces are transmitted at the corresponding point on the ring and a torque is created by the vector of the tangential force leading finally to:

$$\left\{ \begin{array}{l} \underline{F}_r = k\delta l\underline{n} \\ \underline{F}_t = -\frac{k\,\delta l\,(\underline{n}.\underline{t}^{ch})}{(\underline{n}\wedge\underline{e}_Y).\underline{t}^{ch}}.(\underline{n} \wedge \underline{e}_Y) \\ m = F_t\,(l_0 - \delta l) = -\frac{k\,\delta l\,(\underline{n}.\underline{t}^{ch})}{(\underline{n}\wedge\underline{e}_Y).\underline{t}^{ch}}\,(l_0 - \delta l) \end{array} \right. \tag{12}$$

Taking into account the forces determined by (12) and the equilibrium equations (5) of the ring, we can see that $\underline{F}_r, \underline{F}_t$ are functions of variables $(\delta l, \underline{n}, u, w)$. So the unknowns of the equations (5) are $(\delta l, \underline{n}, u, w, \alpha)$. These equations can be written in the following implicit form:

$$\underline{\aleph}(\delta l, \underline{n}, u, w, \alpha) = 0 \tag{13}$$

It is considered that the dynamic configuration is confused with the stationary one of the case of contact with a smooth road. The dynamic equations are deduced from (13) by adding the inertial forces:

$$\left\{ \begin{array}{l} \underline{F^{in}} + \frac{\partial \underline{\aleph}(u_s, w_s, \alpha_s, \delta l_s, \underline{n}_s)}{\partial(u, w, \alpha, \delta l, \underline{n})}(u_t, w_t, \alpha_t, \delta l_t, \underline{n}_t) + \underline{\aleph}(u_s, w_s, \alpha_s, \delta l_s, \underline{n}_s) = 0 \\ z_{li} - f_{ch}(X_{li}) = 0 \\ \delta l > 0 \end{array} \right. \tag{14}$$

Where $\underline{F^{in}}$ is obtained by the terms in second time derivatives and the terms containing Ω in (5). The equations (14) are solved by Newmark's numerical scheme.

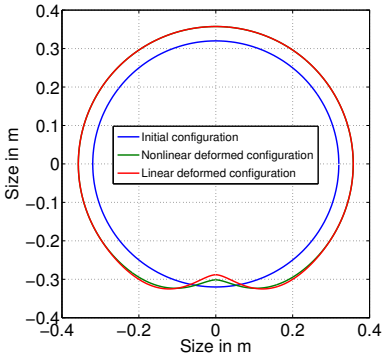

Figure 3: Undeformed and deformed configurations of the tire due to linear and nonlinear static calculations for a point force at the bottom of the tire

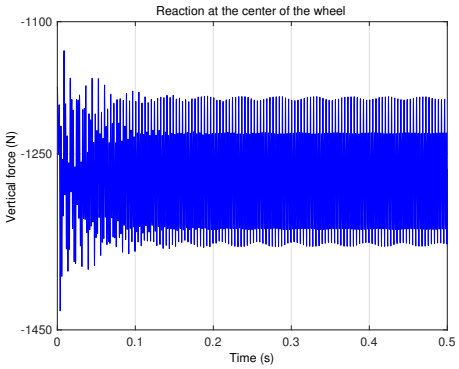

Figure 4: Vertical reaction at the center of the wheel during the dynamic contact on a sinusoidal ground.

4. Validation of models and rotating effects

The dynamic equations are written in the form:

$$\boldsymbol{M}\,\ddot{\boldsymbol{u}}_t + \boldsymbol{C}\,\dot{\boldsymbol{u}}_t + \boldsymbol{K}\,\boldsymbol{u}_t = \boldsymbol{f}_t \tag{15}$$

The matrices $\boldsymbol{M}$ and $\boldsymbol{C}$ are constructed directly using analytical equations. In the case where the effect of large displacements is taken into account, the stiffness matrix $\boldsymbol{K}$ varies during the deformation. Stiffness matrix obtained at the end of the stationary state is the one considered in the dynamic calculation. The model parameters are shown in table (1).

Table 1: Model parameters

Parameter	Description	Value	Unit	Parameter	Description	Value	Unit
E	Young modulus	$2.6611e9$	Pa	ρ	Density	1160.7	kgm^{-3}
R	Ring radius	0.285	m	e	Thickness of the beam	0.01	m
b	Width of the beam	0.085	m	k_R	Radial stiffness	$4.35e6$	Pa
k_θ	Tangential stiffness	$3.19e5$	Pa	ν	Poisson coefficient	0.3	-

The results of the steady state between a Matlab calculation and a calculation under Abaqus are compared at constant boundary conditions and equivalent load and showed good agreement. A comparison of the deformed configurations of the linear case and the nonlinear case in geometry is shown in Figure 3. Near the excitation point one can expect that the stress and strains are large and so in this zone the differences between the linear and non linear models will be the largest.

Figure 4 refers to the vertical force at the center of the wheel during a rolling of the tire on a sinusoidal road at a speed of 10 m/s. This force is computed by the sum of the vertical reactions of the radial springs and the tangential springs between the carcass (the ring) and the wheel center. After a transient phase of a duration of about 1 second, the response becomes periodic. It is mainly the sum of the harmonics of the excitation sine.

Figure 5 shows the associated spectrum. In the ascending order of frequencies, we observe successively tire resonances, the response of the sine of the excitation and the harmonics due to the non linearity of the contact problem. Indeed, the excitation in base of the tire is of sinusoidal form. The excitation frequency is calculated by the ratio of the speed of the ring divided by the wavelength of the road (250 Hz). This sine and its harmonics are present in the stationary response. Moreover, the tire resonances participate in the final response due to the small shocks at the inlet or outlet of the contact area. This is the reason for

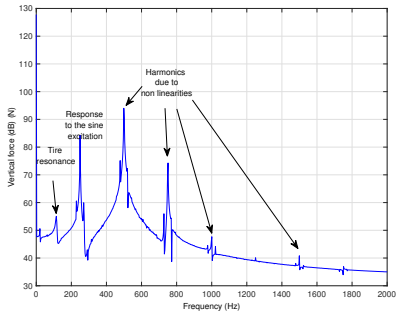

Figure 5: Spectrum of the stationary part of the vertical force at the wheel center during dynamic contact on the sinusoidal ground.

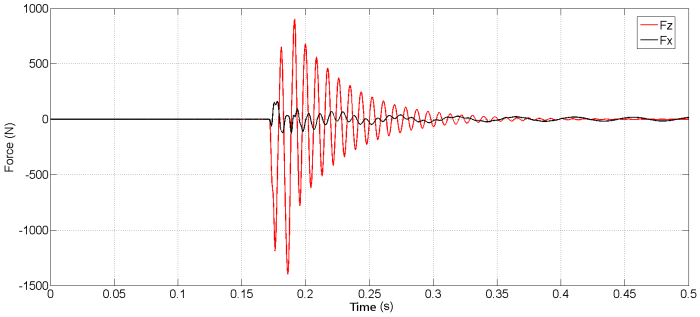

Figure 6: Vertical force and longitudinal force at the wheel center during dynamic contact on a 5 x 10 mm bar for the circular ring.

observing the ring resonances on the spectrum curve. Finally, the contact problem is non linear because the contact area changes at each instant. The non linearity generates periodic harmonics in the response.

In another case, the responses are calculated at the center of the wheel during a rolling on a bar of rectangular section of 5 mm high and 10 mm wide. The temporal responses of the vertical (in red) and longitudinal (in black) forces are plotted in figure 6. As the running speed is 10 m/s, the passage on the bar is very fast (about 0.01s). Thus, the excitation due to the bar can be assimilated to a vertical impact in the base of the tire. It is noted that the level of the vertical force is greater than that of the longitudinal one. The oscillation of the red curve is essentially around the first frequency of the mode of the tire of oval shape (116 Hz).

5. Conclusion

The model developed here allows a good estimation of tire vibrations for low frequencies and includes both linearities coming from the tire behaviour and from the contact with the road. The solution is decomposed into a stationary rolling with a linear dynamic perturbation. Results from rolling on a sinusoidal road or on a bar are given and show the main physical phenomena. Air interior resonance could for instance be added to get a complete model for low frequencies.

References

[1] F. Böhm. Mechanik des gürtelreifens. *Ingenieur-Archiv*, 35(2):82–101, 1966.

[2] M. Heckl. Tyre noise generation. *Wear*, 113(1):157–170, 1986.

[3] W. Kropp. Structure-borne sound on a smooth tyre. *Applied Acoustics*, 26(3):181–192, 1989.

[4] R. Meftah. *Une approche par formalisme de green réduit pour le calcul des structures en contact dynamique: application au contact pneumatique/chaussée*. PhD thesis, Université Paris-Est, 2011.

[5] J. Périsse. A study of radial vibrations of a rolling tyre for tyre–road noise characterisation. *Mechanical systems and signal processing*, 16(6):1043–1058, 2002.

[6] P.H. Campanac, D. Duhamel, and K. Nonami. Modeling of tire vibrations. In *INTER-NOISE 99*, Fort Lauderdale, Florida, USA, December, 06-08 1999.

[7] P.H. Campanac, K. Nonami, and D. Duhamel. Application of the vibration analysis of linear systems with time periodic coefficients to the dynamics of a rolling tyre. *Journal of sound and vibration*, 231(1):37–77, 2000.

[8] S.C. Huang and B.S. Hsu. An approach to the dynamic analysis of rotating tire wheel suspension units. *Journal of sound and vibration*, 156(3):505–519, 1992.

[9] J.M. Muggleton, B.R. Mace, and M.J. Brennan. Vibrational response prediction of a pneumatic tyre using an orthotropic two-plate wave model. *Journal of sound and vibration*, 264(4):929–950, 2003.

[10] J.F. Hamet. Tire/road noise: time domain green's function for the orthotropic plate model. *Acta Acustica united with Acustica*, 87(4):470–474, 2001.

[11] R.J. Pinnington. A wave model of a circular tyre. part 1: belt modelling. *Journal of Sound and Vibration*, 290(1):101–132, 2006.

[12] F. Wullens and W. Kropp. Wave content of the vibration field of a rolling tyre. *Acta Acustica united with Acustica*, 93(1):48–56, 2007.
[13] A. Fadavi. *Modélisation numérique des vibrations d'un pneumatique et de la propagation du bruit de contact*. PhD thesis, Ecole Nationale des Ponts et Chaussées, 2002.
[14] M. Brinkmeier, U. Nackenhorst, S. Petersen, and O. Von Estorff. A finite element approach for the simulation of tire rolling noise. *Journal of Sound and Vibration*, 309(1):20–39, 2008.
[15] Y. Waki, B.R. Mace, and M.J. Brennan. Free and forced vibrations of a tyre using a wave/finite element approach. *Journal of Sound and Vibration*, 323(3):737–756, 2009.
[16] D. Duhamel. A recursive approach for the finite element computation of waveguides. *Journal of Sound and Vibration*, 323(1):163–172, 2009.
[17] D. Duhamel, S. Erlicher, and H.H. Nguyen. A recursive finite element method for computing tyre vibrations. *European Journal of Computational Mechanics*, 20(1-4):9–27, 2011.
[18] M. Brinkmeier and U. Nackenhorst. An approach for large-scale gyroscopic eigenvalue problems with application to high-frequency response of rolling tyres. *Computational Mechanics*, 41(4):503–515, 2008.
[19] I. Lopez, R.E.A. Blom, N.B. Roozen, and H. Nijmeijer. Modelling vibrations on deformed rolling tyres – a modal approach. *Journal of Sound and Vibration*, 307(3-5):481–494, 2007.
[20] I. Lopez, R.R.J.J. van Doorn, R. van der Steen, N.B. Roozen, and H. Nijmeijer. Frequency loci veering due to deformation in rotating tyres. *Journal of Sound and Vibration*, 324(3-5):622–639, 2009.
[21] T.D. Vu, D. Duhamel, Z. Abbadi, H.P. Yin, and A. Gaudin. A nonlinear circular ring model with rotating effects for tire vibrations. *Journal of Sound and Vibration*, 388:245–271, 2017.